Chapter 3

Repair Process after 5-Azacytidine (5AzC)-induced Injury in the Developing Fetal Brain

Introduction

Cytotoxic stresses can induce excessive cell death and suppress cell proliferation in the developing brain (Katayama et al., 2002, 2005a; Ueno et al., 2002a, b, c, 2005; Semont et al., 2004). This damage causes structural abnormalities such as reduction in brain size, disorganization of cortical lamina, and dilatation of the ventricles (Zhang et al., 1995; Sun et al., 1999; Katayama et al., 2000; Kitamura et al., 2001; Furukawa et al., 2004).

Although the mechanisms of fetal brain injury and features of brain abnormalities after birth have been studied, the processes between those stages remain unclear. It is supposed that repair processes are initiated by prenatal damage, because most of the structures of the brain remain after birth even if the fetal brain suffers damage, while some abnormalities are included. Although a few researchers have studied the repair period after damage in the developing brain (Oyanagi et al., 1998; Kikuchi-Horie et al., 2004), it remains unclear how the developing brain responds to the damage, or how the repair process is regulated.

The results in the previous chapters showed that 5AzC induced damage with excess cell death and inhibition of proliferation in the fetal brain. To study the relationship between fetal brain damage and repair, fetal rat brains were exposed to 5AzC, and the resulting recovery and changes in histology and cell proliferation were examined. The role of microglia and cytokines was also investigated in the repair process, since microglial precursors appear in the neuroepithelium at around embryonic day (E) 11 (Ashwell, 1991; Sorokin et al., 1992; Alliot et al., 1999; Kaur et al., 2001), and are

activated in the injured fetal brain (Hao et al., 2001a). Finally, DNA microarray analysis was performed to identify the genes that are activated during the repair process in the developing brain.

Materials and methods

All procedures were approved by the Animal Care and Use Committee of the Graduate School of Agricultural and Life Sciences, The University of Tokyo.

Animals

Pregnant Jcl:Wistar rats were obtained from Japan CLEA . Animals were kept in the same condition as shown in chapter 1.

Chemical

5AzC was obtained from Sigma.

Treatment

On day 13 of gestation, pregnant rats were injected i.p. with 10 mg/kg of 5AzC, and then euthanized at 24, 36, 48, or 60 h after treatment. Control pregnant rats were injected with an equivalent volume of saline, and euthanized at the same time points after treatment.

Histopathology and immunohistochemistry

Collected fetuses were fixed in 10% neutral-buffered formalin and embedded in paraffin. Paraffin sections (thickness, 4 μm) were stained with HE for histopathological examination, or immunostained for ED-1 and Iba-1, markers of microglia, and osteopontin by the LSAB method with streptavidin (Dako). For preparation of frozen sections, fetuses were fixed in 2% periodate-lysine-paraformaldehyde (PLP) for 6 h and then incubated in 15% sucrose/PBS overnight. They were then embedded in O.C.T. compound (Sakura, Tokyo, Japan) and kept at –80 °C until used. Frozen sections (6 μm thick) were used for immunohistochemical staining for ED-1 and CD11b, markers of microglia, by the LSAB method. Mouse anti-ED-1 monoclonal antibody (BMA Biomedicals, Augst, Switzerland), rabbit anti-Iba-1 polyclonal antibody (Wako, Osaka, Japan), mouse anti-CD11b monoclonal antibody (Serotec, Oxford, UK), and rabbit anti-osteopontin (IBL, Fujioka, Japan) were used as the primary antibodies, and biotin-labeled goat anti-rabbit/mouse IgG (Kirkegaard & Perry) as the secondary antibody. Signals were visualized by using a peroxidase–DAB reaction, and the sections were counterstained with methyl green. For double staining, FITC-labeled anti-rabbit IgG (Santa Cruz) and biotin-labeled goat anti-mouse IgG (Kirkegaard & Perry) with rhodamine-labeled avidin (Vector, Burlingame, CA) were used as the secondary antibodies.

TUNEL method

Cells with DNA fragmentation (apoptotic cells) were detected by the TUNEL method using an apoptosis detection kit (Apop Tag; Chemicon, Temecula, CA), as

described in chapter 1.

Lectin staining and electron microscopy

Fetuses were fixed in 4% PFA for light microscopic examination, or 1% PFA/1% glutaraldehyde for electron microscopy, for 6 h, and then incubated in 15% sucrose/PBS overnight. They were then embedded in O.C.T. compound (Sakura) and kept at –80 °C until used. Peroxidase-conjugated BS-I (lectin from *Bandeiraea simplicifolia*; 10 μg/ml: Sigma), was used for detecting microglial cells. Cryosections (thickness, 8 μm) were washed in TBS and placed in 0.3% H_2O_2/methanol for 30 min to inactivate endogeneous peroxidases. Sections were then incubated in 8% skim milk/TBS for 40 min to reduce non-specific staining, and incubated in BS-I overnight at 4 °C. The sections were visualized by a peroxidase-DAB reaction and then counterstained with methyl green. For electron microscopic examination, lectin-stained sections were postfixed in 1% osmium tetroxide in 0.2 M PB for 2.5 h. After dehydration through an ascending ethanol series and propylene oxide, tissues were embedded in Epok 812 resin (Oken). Semi-thin sections were stained with toluidine blue for light microscopic examination. Ultrathin sections were double-stained with uranyl acetate and lead citrate, and observed under a JEOL-1200EX electron microscope (JEOL).

Cell cycle analysis

The telencephalons from two fetuses from each dam (24 to 60 h after treatment) were obtained carefully under stereoscopic microscopy, and divided into two parts, one

containing the dorsal to lateral telencephalic wall and one containing the basal ganglia. They were then prepared for flow cytometric analysis using propidium iodide (PI; 50 μg/ml, Sigma) as described in chapter 1.

RNA extraction, microarray, and data analysis

Microarray expression analysis was performed with the Affymetrix GeneChip system as described in chapter 2. Six to eight fetal telencephalons from each dam (24, 36, or 48 h after treatment, and controls; n = 2 dams per time point) were used for analysis.

Real-time PCR and PCR

Real-time PCR was performed as described in chapter 2. Oligonucleotide primers sets corresponding to the cDNA sequences of *Mif* (NM_031051.1), *Lgals3* (NM_031832.1), *Osteopontin* (AB001382.1), *P4ha1* (BI274401), *Pkm2* (NM_053297.1), *Fgf15* (NM_130753.1), and *Gapdh* were used. Sense and antisense primers were as follows: *Mif-1*, 5′-CAAGCCGGCACAGTACATCG-3′ and 5′-GGT-CGCTCGTGCCACTAAAAG-3′, respectively; *Lgals3*, 5′-GACCACTTCAAGGTT-GCGGTC-3′ and 5′-GGAAGCGCTGGTGAGGGTTAT-3′; *Osteopontin*, 5′-CTGTCT-CCCGGTGAAAGTGG-3′ and 5′-GAGATGGGTCAGGCTTCAGC-3′; *P4ha1*, 5′-CAGGCTGAGCCGAGCTACA-3′ and 5′-CATAGCCAGACAGCCAAGCAC-3′; *Pkm2*, 5′-GGAGGCCAGCGATGGAATC-3′ and 5′- CTGGGTGGCGCAGATGACT-3′; *Fgf15*, 5′-GGGCTGATTCGCTACTCGG-3′ and 5′-GGTGGTGCTTCATGGACC-

TGT-3′; and *Gapdh*, 5′- CCTGCACCACCAACTGCTTAG-3′ and 5′- CATGGACTG-TGGTCATGAGCC-3′. Relative intensity against *Gapdh* was calculated, and the fold change relative to control is shown as the mean ± SD from 3 dams.

PCR was performed as described in chapter 2, using oligonucleotide primer sets corresponding to the cDNA sequences of *TNF-α* (NM_012675.1), *IL-1β* (NM_031512.1), *M-CSF* (AF514356), and *Gapdh*. Sense and antisense primers were as follows: *TNF-α*, 5′-GCTCTTCTGTCTACTGAACTTCG-3′ and 5′-CAGCCTTGT-CCCTTGAAGAGAA-3′, respectively (36 cycles); *IL-1β*, 5′-GATTGCTTCCAAGCC-CTTGACT-3′ and 5′-AGGTGGAGAGCTTTCAGCTCA-3′ (36 cycles); *M-CSF*, 5′-CTCTCCCCATTTTGCCAC-3′ and 5′-TCCTCCGCTTCCAACTGTA-3′ (34 cycles); and *Gapdh*, 5′-GAGTATGTCGTGGAGTCTACTG-3′ and 5′- GCTTCA-CCACCTTCTTGATGTC-3′ (21 cycles).

Results

Histopathological changes

All analyses were performed on the telencephalon, because 5AzC-induced histopathological changes there reflected those in other areas of the central nervous system, including the diencephalon, mesencephalon, and metencephalon (Fig. 1-2B). 5AzC induced apoptosis in the proliferating neural progenitor cells in the VZ, from 6 to 12 h after treatment (Fig. 1-2A, B). Apoptosis was then induced in differentiating neural cells in the DF, outside of the VZ, at 24 h after treatment (Fig. 1-2A-e, 3-1A-b). The number of apoptotic cells peak between 12 and 24 h after treatment (Fig. 1-2B, 2-

3B).

The repair process after 5AzC-induced cell death was examined in two areas of the telencephalon, the telencephalic wall and the basal ganglia (see Fig. I-2A), at various time points between 24 and 60 h. The number of apoptotic cells, defined as cells positive for TUNEL staining, gradually decreased after reaching a peak at 24 h (Figs. 3-1A-b, j, C). Most apoptotic cells were observed in the DF, where postmitotic neural cells are located (arrowheads in Figs. 3-1A-b, d, f, B-b), although there were also some apoptotic cells in the VZ. From 24 to 48 h, many aggregating bodies of apoptotic cells were observed in the VZ and DF (arrowheads in Fig. 3-1B-b, c). At 48 h, the apoptotic cells in the telencephalic wall had almost completely disappeared (Fig. 3-1A-f, C), but were still present in the basal ganglia. By 60 h, apoptotic cells disappeared in the telencephalon, but the thickness of the telencephalic wall was remarkably decreased (Fig. 3-1A-g, h). These results indicate that the recovery from 5AzC-induced damage is completed by around 60 h, and that the process of brain development continues.

Cell cycle analysis

Cell cycle analysis was then performed using flow cytometry to evaluate the proliferation activity after the insult. In the telencephalic wall, many apoptotic cells in the sub-G1 phase were observed at 24 h (control, 0.9 ± 0.1%; 5AzC: 12.6 ± 0.6%), and thereafter the number of apoptotic cells decreased remarkably (Fig. 3-2a, c). The number of S-phase cells increased between 24 and 48 h (Fig. 3-2a, c; control, 24 h: 18.6 ± 0.4%, 36 h: 19.0 ± 1.4%, 48 h: 16.5 ± 0.8%; 5AzC, 24 h: 29.5 ± 5.2%, 36 h: 24.6 ±

4.3%, 48 h: 22.1 ± 0.7%). At 60 h, the distribution of cells in each cell cycle stage recovered close to control levels (Fig. 3-2a, c; control, sub-G1: 0.9 ± 0.1%, G0/G1: 74.3 ± 4.7%, S: 16.9 ± 3.6%, G2/M: 7.9 ± 1.1%; 5AzC, sub-G1: 1.1 ± 0.4%, G0/G1: 72.1 ± 0.8%, S: 17.0 ± 1.4%, G2/M: 9.7 ± 0.2%).

In the basal ganglia, the number of apoptotic cells reached a peak at 36 h (Fig. 3-2b, d; control, 0.6 ± 0.3%; 5AzC: 7.6 ± 0.6%), and then decreased. This peak occurred later than that in the telencephalic wall (12–24 h), and paralleled changes in histopathology (Fig. 3-1C). The proportion of S and G2/M phase cells increased at 48 h (Fig. 3-2b, d; control, S: 8.8 ± 0.3%, G2/M: 5.1 ± 0.9%; 5AzC, 48 h: 13.7 ± 3.0%, G2/M: 8.3 ± 0.3%), and remained slightly elevated at 60 h, although the overall cell cycle distribution was similar to that in controls (Fig. 3-2b, d; control, sub-G1: 0.4 ± 0.1%, G0/G1: 85.2 ± 1.1%, S: 9.0 ± 0.9%, G2/M: 5.4 ± 0.3%; 5AzC, sub-G1: 1.1 ± 0.3%, G0/G1: 81.6 ± 0.2%, S: 11.1 ± 0.1%, G2/M: 6.3 ± 0.1%). These results indicate that the restoration of normal cell cycle control following 5AzC treatment is completed by 60 h, which is consistent with the histopathology results.

Detection of microglia

After E11, amoeboid microglia infiltrate the developing brain from the surrounding tissues, and some of them ingest the apoptotic cells that normally occurred during normal brain development (Ashwell, 1991). These cells are activated by chemical-induced damage (Hao et al., 2001a). To investigate the distribution of microglia in the 5AzC-injured fetal brain, cells were labeled for the microglial markers ED-1, CD11b,

Iba-1, and lectin (BS-I) (Fig. 3-3A; Hao et al., 2001a; Imai and Kohsaka, 2002).

In the control telencephalon, cells positive for Iba-1 or BS-I were observed in the VZ, DF, ventricle, and surrounding mesenchymal tissues (Fig. 3-3A-a). Cells in the ventricle were round, whereas cells in other areas were dendritic or spindle in shape (Fig. 3-3A-a, C-a, D-a). ED-1-positive cells were observed mainly in the mesenchymal tissues around the brain, with only a few positive cells in the telencephalon.

5AzC treatment increased the number of microglia in the telencephalon (Fig. 3-3A-b–f). The number of ED-1-positive cells in the telencephalic wall increased from 24 h after 5AzC-treatment, and that in the basal ganglia increased after 36 h (Fig. 3-3B-a, b). In contrast, the number of Iba-1-positive cells did not increase remarkably in the basal ganglia, but did increase in the telencephalic wall (Fig. 3-3A-a, b; B-c, d), suggesting that 5AzC treatment activates microglia in the basal ganglia, but does not dramatically increase cell proliferation. Indeed, double-staining with ED-1 and Iba-1 showed Iba-1 single-positive cells with ramified morphology in the control basal ganglia (Fig. 3-3C-a), but double-positive cells with amoeboid morphology in the 5AzC group (Fig. 3-3C-b), indicating that injury activates Iba-1-positive microglia, followed by expression of ED-1 and subsequent morphological changes.

The aggregated bodies composed of apoptotic cells were also positive for these markers (Fig. 3-1B-b, c [arrowheads]; 3-3A-e, f, C-b), suggesting that these aggregates are microglia that have ingested apoptotic cells. To confirm this hypothesis, electron microscopy was performed with BS-I staining. Between 24 and 48 h, phagocytotic

cells positive for lectin in the cytoplasmic membrane were observed (Fig. 3-3D-b). Some cells had ingested many apoptotic bodies, indicating that these aggregating bodies were lectin-positive microglia. Their shapes were rounded like amoeboid microglia, whereas dendritic or spindle-type microglia were observed in control brains (Fig. 3-3C-a, D-a).

In the telencephalic wall, most microglia were observed in the DF along the pia mater (Fig. 3-3A-b, c, d), indicating that microglia infiltrated from surrounding mesenchymal tissues. In the basal ganglia, most microglia assembled at the boundary of the VZ and DF, where apoptosis primarily occurred (Fig. 3-3A-b, e, f), whereas they were diffusely distributed in the controls (Fig. 3-3A-a). These results indicate that microglia normally residing in the basal ganglia migrated into the injured area and were transformed into phagocytotic cells.

Expression of cytokines

I determined the expression levels of three cytokines, TNF-α, IL-1β, and M-CSF, that play roles in microglial induction, proliferation, and activation (Nakajima and Kohsaka, 2001; Hao et al., 2001a, b, 2002; Hanisch, 2002). The mRNA levels of all cytokines were up-regulated: *TNF-α* increased between 24 and 60 h, *IL-1β* between 24 and 36 h, and *M-CSF* between 24 and 48 h (Fig. 3-4), suggesting that microglia were activated by these cytokines.

Gene expression in the repair process

DNA microarray analysis was used to determine which genes were modulated by the repair process after 5AzC injury. According to the criteria described in the Materials and Methods, 535 genes were identified (236 genes increased, 299 genes decreased), in which 317 ESTs were included (Table 3-1). Genes categorized by GenMAPP as important in glial cells, inflammation (response to wounds), the extracellular matrix, glycolysis, and neural development were upregulated (Table 3-1). Real-time PCR was used to confirm the mRNA expression levels of several genes that showed changes in the DNA microarray analysis.

The microglial marker Iba-1 was upregulated at 24 h, which is consistent with the results that Iba-1-positive microglia increased (Fig. 3-3A, B). Other markers of cells from macrophage lineages, Lgals3/Galectin3, Mif, and osteopontin (Walther et al., 2000; Imai and Kohsaka, 2002; Calandra and Roger, 2003; Sano et al., 2003; Choi et al., 2004), were also upregulated between 24 and 36 h (Table 3-1). The elevated expression was confirmed by real-time PCR (Fig. 3-5A). Osteopontin staining was detected in phagocytic microglial cells that co-expressed ED-1 (Fig. 3-5B). Further, various genes related to response to wounds (inflammation) were upregulated from 24 to 36 h (Table 3-1), suggesting that, even in the developing brain, the inflammatory response is induced by injury. Indeed, the elevated expression of three cytokines, IL-1β, M-CSF, and TNF-α, that are related to inflammation and microglial activation, was detected as mentioned above (Fig. 3-4). The upregulation of these cytokines in the DNA microarray analysis could not be detected, because IL-1β and M-CSF were not present in the microarray used in this study, and the expression of TNF-α was too low

to evaluate.

The expression of genes involved in regulating the extracellular matrix and glycolysis was elevated between 24 and 48 h (Table 3-1). The upregulation of *P4ha1*, the gene for an enzyme for collagen synthesis, and *Pkm2*, encoding a glycolytic enzyme, were confirmed with real-time PCR (Fig. 3-5C-a, b), which supports the microarray data showing that these genes were changed by 5AzC treatment. The expression of genes related to neural development was also changed between 24 and 48 h (Table 3-1). It was confirmed that the expression of Fgf15, a growth factor important for brain development, was also elevated with real-time PCR (Fig. 3-5C-c).

The expression of genes involved in proliferation, cell cycle control, and apoptosis was also changed between 24 and 48 h (Table 3-1). These changes may be related to the cell cycle alterations after 5AzC treatment, or may be important in the recovery of proliferation.

Discussion

Extrinsic stresses can negatively affect brain development. Treatment with cytotoxic chemicals leads to apoptotic cell death in fetal brain and brain malformation in neonatal pups. However, the developmental process seems to continue after injury, as was shown by the present histopathologic examination (Fig. 3-1) and analysis of cell cycle kinetics (Fig. 3-2), indicating that the fetal brain maintains the capacity for repair and recovery.

Regulation of proliferation and regeneration

The number of S-phase cells increased from 24 to 48 h after 5AzC-treatment, similar to the results indicating observed some increase of BrdU-positive S-phase cells in the VZ at 24 h (Fig. 1-3A-g, B). It is reported that like 5AzC, ethylnitrosourea (ENU), a DNA damaging agent also causes neuroepithelial cells to synchronize in the S phase during recovery and then return to normal proliferation (Oyanagi et al., 1998) and this suggests that DNA repair might be coincident with S-phase retardation. Further, these results suggest that damage initiates regeneration more easily in the developing brain than in adults. While the adult brain can reproduce neurons, astrocytes, and oligodendrocytes after brain injury (Magavi et al., 2000; Doetsch, 2003), the degree of regeneration is not large. On the other hand, regeneration occurs rapidly after damage to the developing brain (Shimada and Langman, 1970; Houle and Das, 1983; Oyanagi et al., 1998), which is consistent with the present results. Thus, the present experimental model may offer important information on the mechanisms of brain regeneration.

The role of microglia

The present results showed that brain injury stimulated microglia to participate in the repair process by clearing dead cells. These microglia could have originated intrinsically, because microglia are present in the brain after E11 (Ashwell, 1991), or infiltrated from the surrounding mesenchymal areas, blood vessels, or ventricles, as suggested by their presence near the pia mater of the telencephalic wall (Fig. 3-3A). Indeed, these tissues are the sources of the monocytes and hematopoietic cells that

eventually form microglia (Sorokin et al., 1992; Cuadros and Navascues, 1998; Kaur et al., 2001), although some studies indicate that microglia can also arise partly from a neuroepithelial lineage (Cuadros and Navascues, 1998).

Changes in gene expression profiles were analyzed by using DNA microarrays and upregulated genes important in glial cells, and inflammation, which is supposed to be related to microglial functions, were identified. *Iba-1* and *Lgals3/Galectin3* are both expressed in phagocytotic cells (Walther et al., 2000; Imai and Kohsaka, 2002; Sano et al., 2003), indicating that infiltrating microglia express these genes. Indeed, the number of *Iba-1*-positive microglia increased dramatically after injury (Figs. 3-3A-b, B-c). Moreover, I found elevated levels of markers for two other types of glial cell, oligodendrocytes and astrocytes. The expressions of *Olig-1* (Zhou et al., 2000) and *Fgfr3* (Bansal et al., 2003), markers of oligodendrocyte precursors, were elevated, although their role in the present study remains unclear. Glast-1 is a glutamate transporter whose gene is expressed in astrocytes in the adult brain, as well as on neural progenitor cells (radial glia) in the developing brain (Hartfuss et al., 2001). It could not be determined whether the increase observed in this marker was due to increased expression by individual cells, or to an increased number of neural progenitor cells expressing *Glast-1*. Microglia and astrocytes primarily mediate the repair of lesions in the adult brain (Fawcett and Asher, 1999). However, any GFAP-positive astrocytes could not be detected in this model (data not shown), because the astrocytes derived from neural progenitor cells are generated later in development (Qian et al., 2000; Takizawa et al., 2001; Sun et al., 2003; Namihira et al., 2004).

Some genes involved in inflammation were also upregulated during the repair process, suggesting that these neural cells have a capacity to respond to damage and to initiate the repair process, followed by the activation of microglia. Osteopontin is expressed on amoeboid microglia in the developing brain, and is important in regulating migration and phagocytosis (Choi et al., 2004). Here I found that the expression of *Osteopontin* mRNA was upregulated, and that protein production was detected in phagocytotic amoeboid microglia (Fig. 3-5B). ENU-induced brain damage also leads to upregulation of *Osteopontin* during the recovery phase (Katayama et al., 2005b), suggesting that Osteopontin may play an important role in the repair of the developing brain. In addition, I found increased expression levels of three cytokines involved in the activation of microglial cells, TNF-α, IL-1β, and M-CSF (Fig. 3-4), as well as increases in Mif (Table 3-1 and Fig. 3-5A-b), a cytokine with proinflammatory effects (Calandra and Roger, 2003). The respective genes play roles in the induction, proliferation, and activation of microglia (Nakajima and Kohsaka, 2001; Hanisch, 2002), and their expression is upregulated by CP-induced injury to fetal brains (Hao et al., 2001a). TNF-α is expressed in microglia and neural progenitor cells, and CSF-1R, encoding an M-CSF receptor, in microglial cells (Hao et al., 2001a, b, 2002). These reports indicate the importance of these cytokines for activating microglial cells. It is known that microglia release two types of opposing signaling molecules, cytotoxins and neurotrophic factors (Nakajima and Kohsaka, 2001), so their effects on damaged tissue change depending on the local environment. Further investigation of microglial function in this model is needed to clarify their role.

Gene expression in the repair process

Upregulated genes important in the extracellular matrix, glycolysis, and neural development were identified in the DNA microarray analysis, and many genes were found to be regulated in response to chemical-induced damage and the subsequent recovery.

The extracellular matrix is important in the remodeling that occurs after tissue damage. 5AzC-treatment increased the gene expression of various types of collagen, laminin, and proteases (Table 3-1). Glycolysis is usually induced under hypoxic conditions. Chemical injury might induce hypoxia-like conditions, causing neural progenitor cells to upregulate glycolytic genes. Hypoxia-inducible factors (HIFs) are the key transcription factors that respond to hypoxic conditions and control various target genes related to vascularization, glucose uptake/glycolysis, erythropoiesis, etc. (Bracken et al., 2003; Michiels, 2004). Elevated expression of two HIF targets, *P4ha1* and *Pkm2* was observed (Fig. 3-5C-a, b) (Bracken et al., 2003). Further work is necessary to examine the expression of these transcription factors.

The expression of genes related to neural development was changed during the repair process, suggesting that tissue remodeling occurred. The normal, controlled expression patterns of these genes during brain development are critical for the formation of the complicated regional patterning of the brain (Rubenstein et al., 1998, Grove and Fukuchi-Shimogori, 2003). Expression changes in patterning-related genes that are expressed in a restricted region of the telencephalon, including *Fgf15* (Gimeno

et al., 2003), *Lhx5* (Sheng et al., 1997), *Lhx2* (Monuki et al., 2001), *Dlx5* (Eisenstat et al., 1999), and *BF-1* (Dou et al., 1999) were observed. Other genes are targets of the brain signaling molecules, Wnt, Fgf, and Shh, which play critical roles in the proliferation, differentiation, and patterning of the developing brain (Altmann and Brivanlou, 2001; Salie et al., 2005). For example, Lef1 is a transcription factor in the Wnt signaling pathway (Galceran et al., 2000), Fgfr3 is an Fgf receptor (Johnson and Williams, 1993; Bansal et al., 2003), and the expression of *Fgf15* is induced by Shh (Saitsu et al., 2005). It is unclear whether these changes in expression reflect changes in cell populations expressing the genes, or whether they reflect mechanisms controlling the proliferation, differentiation, and patterning in response to tissue damage, but it would be interesting to examine the sequential changes of these expression patterns in more detail.

I show here that the developing brain has the capacity to respond to the damage induced by extrinsic chemical stresses, including changing the expression of numerous genes and recruiting microglia to aid the repair process (Fig. 3-6). The degree of damage induced by extrinsic stresses, and the extent of the subsequent repair process, would dramatically influence the level of abnormalities that would come in the neonatal brain. My present results offer important insights into the mechanisms of repair and regeneration in the developing brain.

Summary

The developing fetal brain is susceptible to many extrinsic stresses. Some of these stresses induce excessive cell death, leading to anomalies in the neonatal brain. However, it is unclear how the developing brain responds and adapts to the tissue damage. Pregnant rats on day 13 of gestation were treated with 5AzC to damage the fetal brain, and investigated the repair process up to 60 h after treatment. Histological analysis showed that 5AzC induced strong apoptosis of neural cells. By 60 h, apoptotic cells disappeared and the tissue was repaired, although the telencephalic wall remained thinner than that in controls. Flow cytometry analysis showed that the cell cycle distribution also returned to control levels at 60 h, suggesting that the repair process was completed around 60 h. During the repair period, amoeboid microglia infiltrated the brain and ingested the apoptotic cells. These microglial cells were positive for the microglial markers, ED-1, Iba-1, CD11b, and BS-I. Further, mRNAs for the microglia-related cytokines, TNF-α, IL-1β, and M-CSF, were upregulated. DNA microarray analysis showed the upregulation of genes relevant to glial cells, inflammation, the extracellular matrix, glycolysis, proliferation, and neural development. The present results showed that the developing brain has the capacity to respond to the damage induced by extrinsic chemical stresses, including changing the expression of numerous genes and the induction of microglia to aid the repair process.

Accession No.	Genes	Fold change 24 h	36 h	48 h
Glial Cell				
NM_017196.1	Iba-1/ allograft inflammatory factor 1 (Aif1)	1.85±0.58		
NM_031832.1	lectin, galactose binding, soluble 3 (Lgals3) / galectin-3 / Mac2	1.85±0.31	3.42±1.1	
NM_021770.2	oligodendrocyte transcription factor 1 (Olig1)		1.83±0.47	
AF265360.1	GLAST-1a / solute carrier family 1. member 3 (Slc1a3)		1.77±0.02	1.61±0.38
Inflammation / Response to wounds				
NM_053843.1	Fc receptor, IgG, low affinity III (Fcgr3)		1.67±0.06	
NM_012512.1	Beta-2-microglobulin (B2m)		1.55±0.16	
AI169104	platelet factor 4 (PF4) / small inducible cytokine subfamily B, member 4 (Scyb4) / Cxcl4	1.71±0.08		
NM_019905.1	calpactin I heavy chain (Anxa2)	1.49±0.28		
AI411582	zyxin (Zyx)	1.48±0.32		
BI284441	ESTs, Weakly similar to kupffer cell receptor (Kucr) / C-type lectin 13	1.43±0.03		
AI407114	EST (complement component 3)	1.38±0.10		
NM_017200.1	tissue factor pathway inhibitor (Tfpi)	1.32±0.01		
NM_013087.1	CD81 antigen (Cd81)	1.32±0.01		
NM_031051.1	macrophage migration inhibitory factor (Mif)	1.36±0.03	1.68±0.03	
AB001382.1	osteopontin / secreted phosphoprotein 1 (Spp1)		2.30±0.43	
AI411618	ESTs, Weakly similar to complement c1q subcomponent, B chain precursor		1.59±0.03	
BF285771	ESTs, Highly similar to mouse Rho GDP-dissociation inhibitor 2		1.48±0.09	
BE111722	ESTs, Highly similar to high affenity immunoglobulin epsilon receptor gamma-subunit precursor (Fceg)		1.38±0.01	
NM_017113.1	granulin (Grn)		1.32±0.19	
AI409182	ESTs, Weakly similar to ADP-ribosylation factor (Arf3)		1.24±0.01	
BM383427	Interleukin 6 signal transducer (Il6st) / gp130 transducer chain (gp130)			1.51±0.01
NM_022297.1	dimethylarginine dimethylaminohydrolase 1 (Ddah1)	-1.28±0.03		
NM_017165.1	glutathione peroxidase 4 (Gpx4)	-1.22±0.02		
NM_012889.1	vascular cell adhesion molecule 1 (Vcam1)	-1.78±0.07	-1.85±0.24	
BE111083	ESTs, Highly similar to mouse complement-activating component of RA-reactive factor precursor (Crar)			-1.51±0.14
BI285183	thymus cell surface antigen (Thy1)			-1.72±0.85
BI276424	ESTs, Highly similar to mouse vacuolar ATP synthase subunit D (VA0D) / physophilin			-1.30±0.11

Accession No.	Genes	Fold change 24 h	36 h	48 h
Extracellular Matrix				
BM390457	TGF-beta masking protein large subunit (Ltbp1)	2.04±0.52		
NM_024400.1	a disintegrin and metalloproteinase with thrombospondin motifs 1 (Adamts1)	1.67±0.06		
BI275624	laminin, gamma 1 (Lamc1)	1.32±0.01		
BM388837	procollagen, type I, alpha 2 (Col1a2)	1.26±0.04		
BI285575	procollagen, type I, alpha 1 (Col1a1)	1.24±0.01		
BI274401	prolyl 4-hydroxylase alpha subunit (P4ha1)	1.50±0.05	1.36±0.19	
Z78279.1	collagen alpha1 type I (Col1a1)		1.31±0.15	
NM_012656.1	secreted acidic cystein-rich glycoprotein (Sparc) / osteonectin		1.24±0.13	
AF305418.1	type II collagen (Col2a1)		1.39±0.04	1.71±0.21
BE111752	ESTs, Highly similar to mouse procollagen alpha 1 (IV) precursor			1.65±0.17
AI171185	hyaluronan mediated motility receptor (Hmmr / Rhamm)			1.51±0.02
BI275716	procollagen, type III, alpha 1 (Col3a1)			1.37±0.07
AI179127	small proteoglycan I / biglycan (Bgn) / bonecartilage proteclycan 1 precursor			-1.56±0.47
L38247.1	synaptotagmin IV			-1.33±0.02
L20468.1	cerebroglycan / glypican-2 (Gpc2)			-1.33±0.08
NM_019907.1	postsynaptic protein Cript (Cript)			-1.23±0.10
Glycolysis				
BM389769	Highly similar to 6-phosphofructokinase	1.85±0.64		
NM_053290.1	phosphoglycerate mutase 1 (Pgam1)	1.30±0.03		
NM_030834.1	monocarboxylate transporter (Mct3) / Slc16a8	2.22±0.07	1.90±0.26	
NM_013190.1	phosphofructokinase, liver, B-type (Pfkl)	1.43±0.02	1.74±0.21	
NM_017025.1	lactate dehydrogenase A (Ldha)	1.40±0.11	1.68±0.45	
BI283882	ESTs, Highly similar to mouse glucose-6-phosphate isomerase	1.34±0.04	1.63±0.29	
NM_053297.1	pyruvate kinase 3 (Pkm2) / pyruvate kinase, isozymes M1/M2	1.21±0.01	1.35±0.03	
AI548699	ESTs, Highly similar to mouse galactokinase		1.84±0.55	
NM_012495.1	aldolase A, fructose-bisphosphate (Aldoa)		1.44±0.21	
NM_053291.1	phosphoglycerate kinase 1 (Pgk1)		1.39±0.20	
NM_012554.1	enolase 1, alpha (Eno1)		1.38±0.02	
AA848319	lactate dehydrogenease B (Ldhb)	-1.4±0.10		
Neural development				
NM_130753.1	fibroblast growth factor 15 (Fgf15)	1.73±0.25		
NM_031601.1	calcium channel, voltage-dependent, T type, alpha 1G subunit (Cacna1g)	1.37±0.11		

Accession No.	Genes	Fold change 24 h	36 h	48 h
BF283398	EST (chemokine (C-X-C motif) ligand 12)	1.23±0.02		
NM_019161.1	cadherin 22 (Cdh22)	2.06±0.10	2.37±0.6	
BI274355	Weakly similar to neuronal olfactomedin-related ER localized protein precursor (Nomr) / Noelin / Olfactomedin 1(Olfm1) / Pancortin	1.61±0.04	1.48±0.16	
BI274903	ESTs, Moderately similar to tubulin beta chain 15	1.37±0.09	1.49±0.20	
NM_053744.1	delta-like homolog (Dlk1) / Pref-1	1.60±0.13	2.08±0.70	1.85±0.11
J02582	apolipoprotein E (ApoE)		1.50±0.06	
BI283479	ESTs, Weakly similar to LIM homeobox protein (Lhx5)		1.42±0.17	
BG671569	ESTs, Weakly similar to drome out at first protein (Oaf)		1.36±0.01	
NM_130429.1	lymphoid enhancer binding factor 1 (Lef1)		1.42±0.06	
NM_053429.1	fibroblast growth factor receptor 3 (Fgfr3)			1.59±0.19
NM_053936.1	endothelial differentiation, lysophosphatidic acid G-protein-coupled receptor, 2 (Edg2)			1.43±0.08
BE113437	neural plakophilin related arm-repeat protein (Nprap) / catenin, delta-2 (Ctnnd2)			1.34±0.08
NM_030856.1	neuronal leucine-rich repeat protein-3 (Lrrn3)	-1.62±0.21		
M55292.1	neural receptor protein-tyrosine kinase (TrkB)	-1.56±0.06		
NM_024383.1	hairy and enhancer of split 5 (Hes5)	-1.53±0.13		
L06804.1	LIM homeodomain protein (Lhx2 / Lh-2)	-1.43±0.04		
NM_012943.1	distal-less homeobox (Dlx5)	-1.35±0.03		
NM_012560.1	Forkhead-like transcription factor Bf-1 (Fkhr)	-1.34±0.03		
NM_053583.1	Olf-1EBF associated Zn finger protein Roaz (Roaz)	-1.37±0.09	-1.35±0.05	
AW144823	ESTs, Highly similar to mouse SorLA precursor (Sortilin-related receptor precursor)		-1.57±0.14	
NM_053346.1	neuritin (Nrn)		-1.51±0.09	-1.40±0.15
BG668493	superiorcervical ganglia, neural specific 10 (Scgn10) / stathmin-like 2 (Stmn2)			-1.54±0.38
NM_053654.1	platelet-activating factor acetylhydrolase, isoform 1b, alpha1 subunit (Pafah1b3)			-1.53±0.45
L20468.1	cerebroglycan / glypican-2 (Gpc2)			-1.33±0.08
NM_024147.1	Rnb6 (Evl/Ena/vasodilator stimulated phosphoprotein-like protein (Ena/VASP-like protein))			-1.29±0.15
Cell Cycle / Proliferation				
NM_012588.1	insulin-like growth factor-binding protein (Igfbp3)	2.30±0.43		
BE106888	ESTs, Weakly similar to epidermal growth factor precursor (Egrt)	1.38±0.09		
BM391890	ESTs, Highly similar to human CAD protein (PYR1)	1.34±0.07		

Accession No.	Genes	Fold change 24 h	36 h	48 h
NM_133298.1	glycoprotein (transmembrane) nmb (Gpnmb) / osteoactivin	3.03±0.15	3.16±0.74	3.41±0.10
NM_012760.1	Lost on transformation 1 (Lot1)	1.47±0.14	1.94±0.07	1.98±0.15
M86708.1	inhibitor of DNA binding (Id1)		1.65±0.29	
NM_017113.1	granulin (Grn)		1.32±0.19	
NM_030859.1	midkine (Mdk)		1.28±0.04	
AI714002	ESTs, Moderately similar to mouse Ki-67			1.58±0.19
AW533924	exportin 1 (Xpo1 / Crm1, yeast, homolog)			1.52±0.26
NM_134472.2	kinesin-related protein 2 (Krp2) / kinesin-like protein (Kif2c) / mitotic centromere-associated kinesin (Mcak)			1.35±0.10
NM_012514.1	breast cancer 1 (Brca1)			1.28±0.09
AA848420	ESTs, Highly similar to mouse uracil-DNA glycosylase precursor (Ung)	-2.01±0.2		
AI599423	ESTs, Highly similar to growth arrest and DNA-damage-inducible protein (Gadd45 gamma)	-1.91±0.05		
NM_019348.1	somatostatin receptor subtype 2 (Sstr2)	-1.62±0.01		
AI412150	ESTs, Weakly similar to DNA-binding protein inhibitor (Id2)	-1.57±0.12		
NM_022381.1	proliferating cell nuclear antigen (Pcna)	-1.32±0.02		
BI288701	B-cell translocation gene 2, anti-proliferative (Btg2)	-1.29±0.10		
NM_012755.1	Fyn proto-oncogene (Fyn)	-1.17±0.03		
AY043246.1	regulator of G-protein signaling 2 (Rgs2)	-1.53±0.07		-1.40±0.11
NM_031762.1	cyclin-dependent kinase inhibitor 1B (Cdkn1b, p27, Kip1)		-1.63±0.23	
BM389730	ESTs, Moderately similar to mouse DNA topoisomerase II, beta isozyme (Tp2b)		-1.30±0.10	
AI233712	ESTs, Highly similar to mouse protein phosphatase 2C delta isoform (Pp2c-delta)		-1.24±0.05	
BE113079	ESTs, Weakly similar to nucleolin (Nucl)			-1.55±0.22
AA944459	dynein light intermediate chain 1			-1.34±0.11
NM_031821.1	serum-inducible kinase (Snk)			-1.33±0.25
NM_017258.1	B-cell translocation gene 1, anti-proliferative (Btg1)			-1.26±0.02
Apoptosis				
BE112895	ESTs, Weakly similar to mouse mammary transforming protein	-1.38±0.09		
NM_017165.1	glutathione peroxidase 4 (Gpx4)	-1.22±0.02		
U84410.1	interleukin-1beta-converting enzyme-related protease (Cpp32) / caspase 3 (Casp3)		-1.26±0.14	
AI102437	zinc finger protein RP-8 / programmed cell death protein 2			-1.63±0.40

Accession No.	Genes	Fold change 24 h	36 h	48 h
AF441118.1	BNIP3L protein (Bnip3l) / Bcl2			-1.51±0.22
NM_133561.1	brain protein 44-like (Brp44l) / apoptosis-regulating basic protein			-1.66±0.62

Table 3-1. Gene expression changes during the repair period of the rat fetal telencephalon after 5AzC treatment. Fold change is presented as the mean ± SD of 2 arrays.

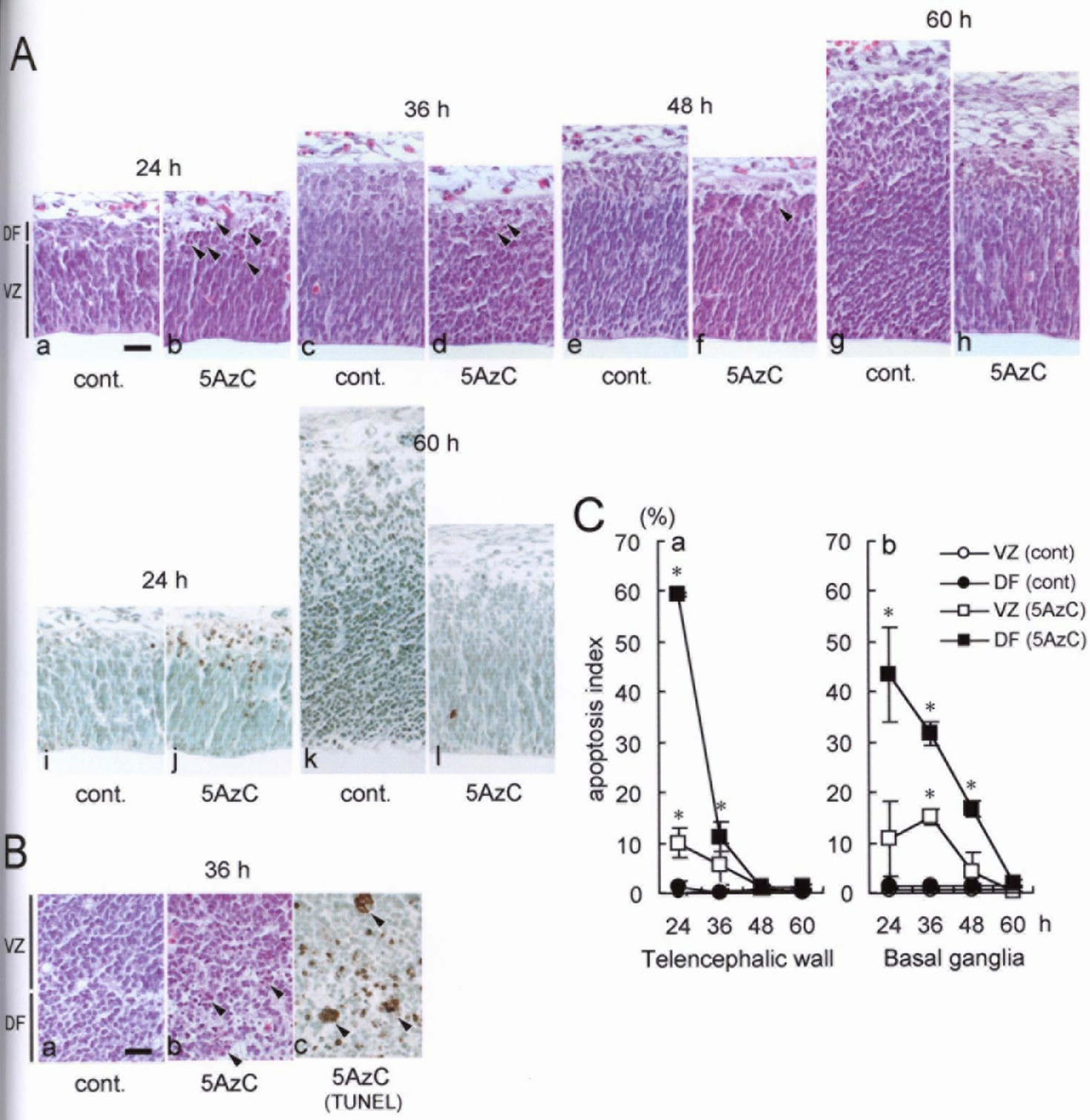

Fig. 3-1. Histopathological changes through the repair period in the telencephalon of 5AzC-treated rat fetuses. A: The telencephalic wall (a, b, i, j: 24 h; c, d: 36 h; e, f: 48 h; g, h, k, l: 60 h) was stained by HE (a–h) or TUNEL (i–l). At each timepoint, the left panel is the control and the right panel is 5AzC-treated tissue. Apoptotic cells were observed mainly in the DF (arrowheads in b, d, and f). The thickness of the telencephalic wall was remarkably decreased at 60 h (g, h). Scale bar: 50 μm. B: The basal ganglia (36 h) were stained by HE (a, b) or TUNEL (c). a: control; b, c: 5AzC-treated group. Aggregating bodies of apoptotic cells were observed (arrowheads in b and c). Scale bar: 50 μm. C: Apoptosis index. TUNEL-positive apoptotic cells were counted in the VZ (open) and DF (closed) of control (circle) and 5AzC-treated (square) telencephalic wall (a) and basal ganglia (b). The apoptosis index (%; the number of TUNEL-positive cells/500 cells) represents the mean ± SD of 3 dams. *: $p < 0.05$; significantly different from control (Student's *t*-test).

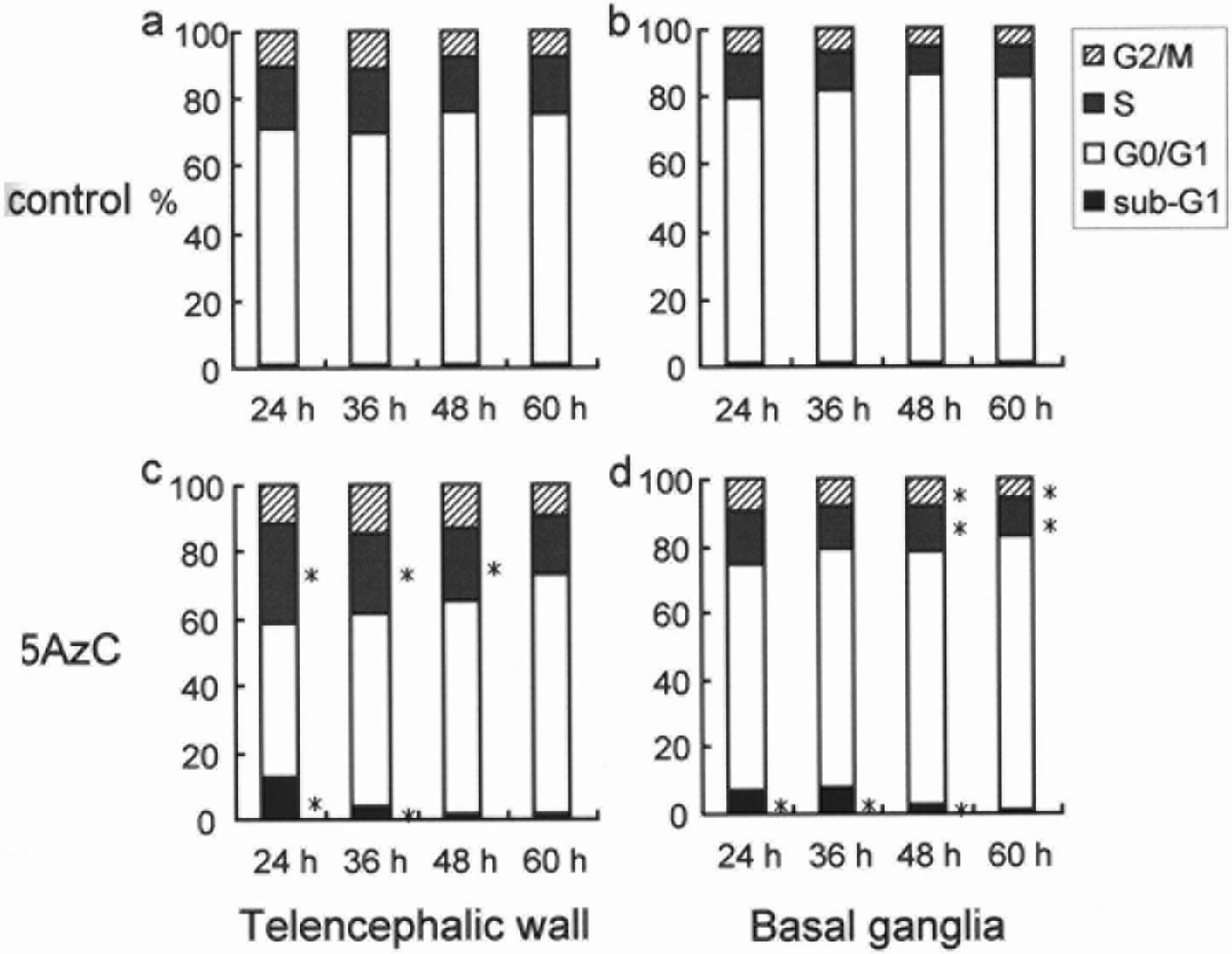

Fig. 3-2. Cell cycle analysis of telencephalic cells in the rat fetus (a, c: telencephalic wall; b, d: basal ganglia; top panel: control; bottom panel: 5AzC-treated). Percentages for each cell cycle phase are presented as the mean of 3 dams (hatched bar: G2/M; gray bar: S; white bar: G0/G1; black bar: sub-G1). 5AzC-treatment increased the number of S-phase cells and apoptotic cells in the sub-G1 area, and cell cycle distribution returned close to control levels at 60 h. *: $p < 0.05$; significantly different from control (Student's *t*-test).

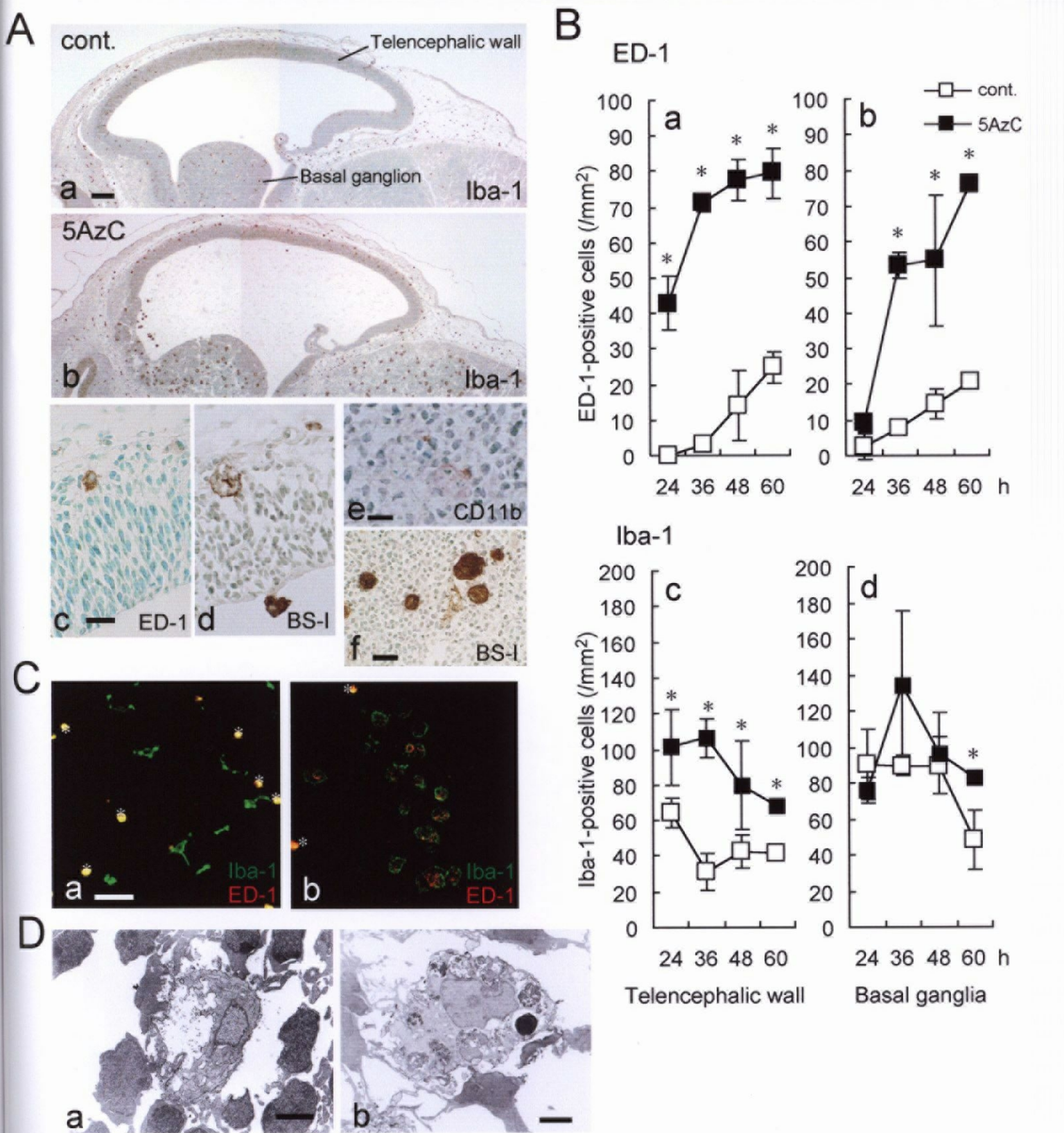

Fig. 3-3. Infiltration and activation of microglia in the 5AzC-treated telencephalon. A: Detection of microglia with several immunohistochemical markers (a: control; b–f: 5AzC-treated) at 36 h after treatment. a, b: Iba-1; c: ED-1; d, f: BS-I; e: CD11b. a, b: telencephalon (telencephalic wall and basal ganglion), c, d: telencephalic wall; e, f: basal ganglia. Scale bar: 150 μm (a, b), 50 μm (c–f). B: Microglial cell index. ED-1- (a, b) and Iba-1- (c, d) positive microglia were counted in control (white square) and 5AzC-treated (black square) telencephalic wall (a, c) and basal ganglia (b, d). *: $p < 0.05$: significantly different from the control group (Student's *t*-test). The number of marker-positive cells increased except for Iba-1-positive cells in basal ganglia (d). C: Double staining of Iba-1 (green) and ED-1 (red) in control (a) and 5AzC-treated (b) basal ganglia at 36 h. Iba-1-positive ramified microglia were observed in control tissue (a). In 5AzC-damaged tissue, activated amoeboid microglial cells expressed both Iba-1 and ED-1 (b). The asterisks show blood cells that were nonspecifically labeled. Scale bar: 50 μm. D: Electron micrograph with lectin (BS-I) staining. Dendritic or spindle cell in control (a), and a rounded cell that has phagocytized apoptotic cells in the 5AzC-treated telencephalon (b). Lectin staining in the membrane is shown as a black signal. Scale bar: 2 μm.

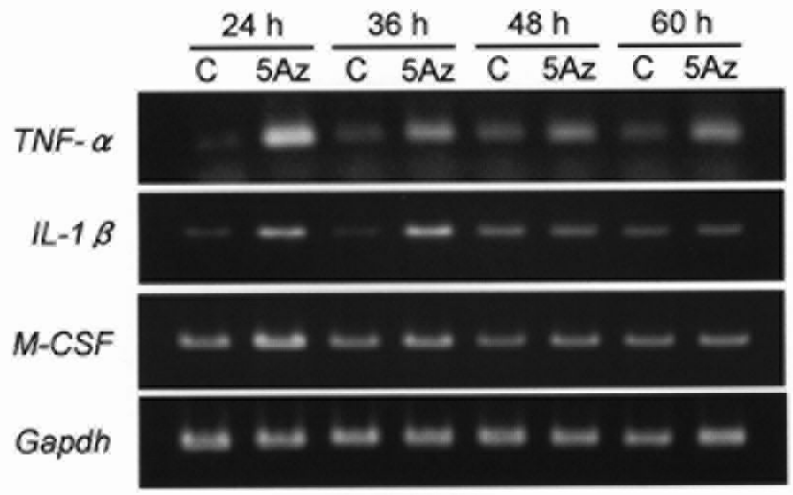

Fig. 3-4. Expression of cytokines important in the induction, proliferation, and activation of microglial cells. C: control group, 5Az: 5AzC-treated group. Levels of *TNF-α*, *IL-1β*, and *M-CSF* mRNA were detected by RT-PCR. Their expression was elevated between 24 and 60 h. *Gapdh* was included as an internal control.

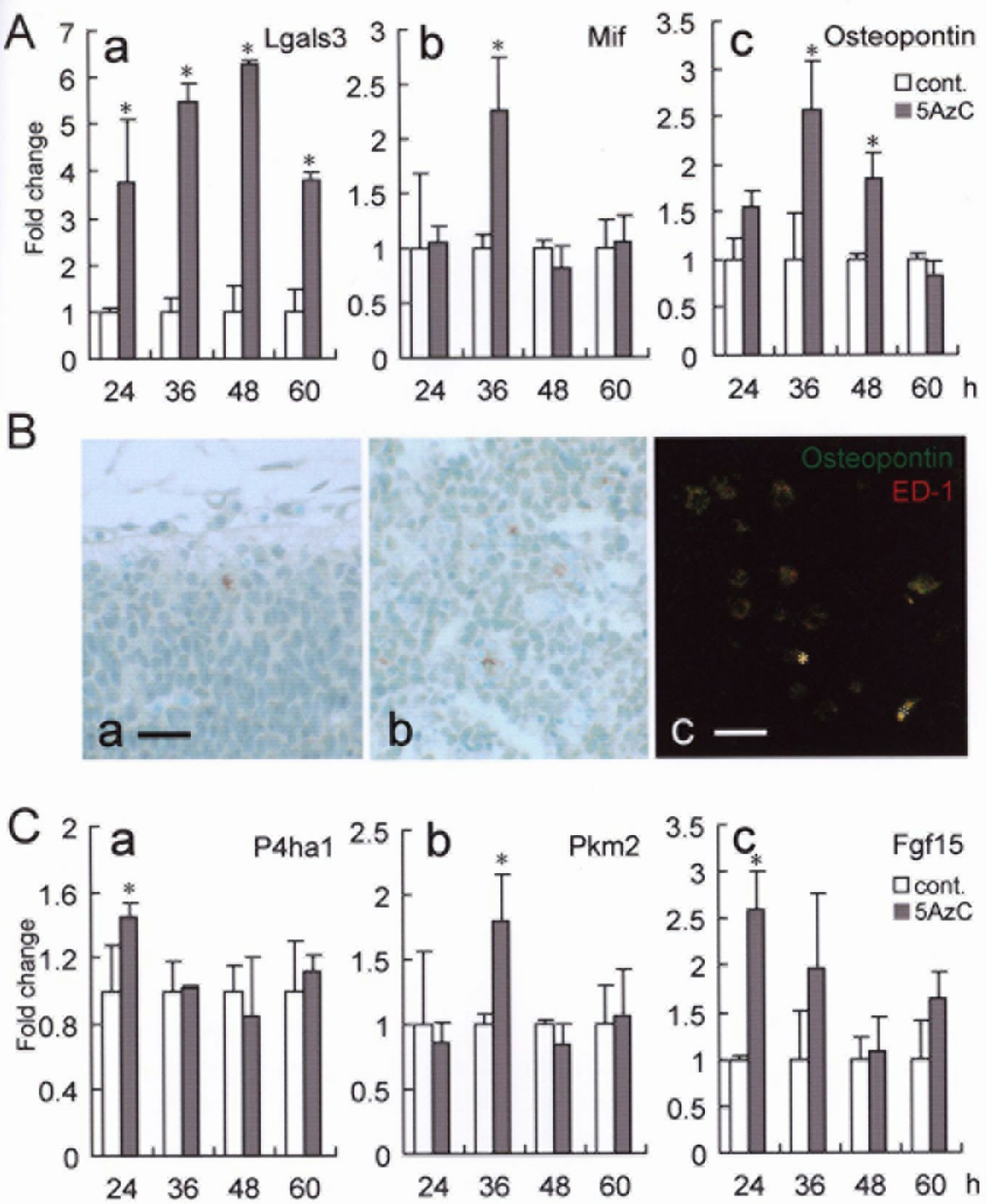

Fig. 3-5.. The expression of genes during the repair period. A: The expression of genes related to microglia and inflammatory responses (responses to wounding). mRNA levels of *Lgals3* (a), *Mif* (b), and *Osteopontin* (c), which were upregulated in the DNA microarray analysis (Table 3-1), were detected by real-time PCR. White bar: control; gray bar: 5AzC-treated group. Fold change relative to control is represented as the mean ± SD of 3 dams. Increases in expression were consistent with the results of the DNA microarray analysis (Table 3-1). *$p<0.05$; significantly different from control (Studnt's t-test). B: Osteopontin-labeled microglia in the 5AzC-treated telencephalon. a: telencephalic wall; b, c: basal ganglia; 36 h after 5AzC treatment. Microglial cells were double-labeled for osteopontin (green) and ED-1 (red) (c). The asterisks show blood cells that were nonspecifically labeled. Scale bar: 50 μm. C: Expression of genes important in the extracellular matrix, glycolysis, and neural development. The expression of *P4ha1* (a; extracellular matrix), *Pkm2* (b; glycolysis), and *Fgf15* (c; neural development) was examined by real-time PCR. The representations are similar to those in A.

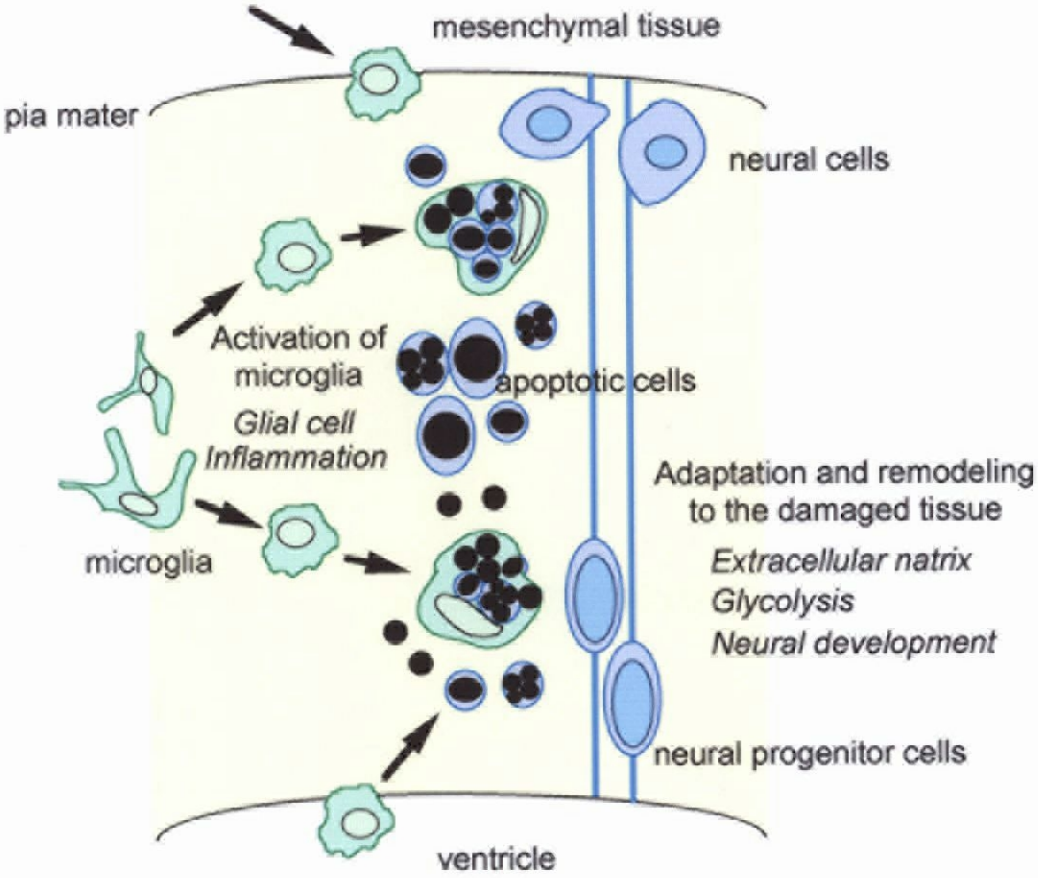

Fig. 3-6. Developing brain responds to the tissue damage induced by 5AzC, including changing the expression of numerous genes and the induction of microglia to aid the repair process. Blue cells: developing neural cells, green cells: microglia. Categories of elevated genes are represented as an italic type. After tissue damage, residing dendritic or ramified microglia are activated and become rounded and phagocytotic, which ingest apoptotic cells. Microglia also infiltrate from surrounding tissues, mesenchymal tissues through pia mater and ventricle. Inflammatory genes may contribute to these processes. The expression of genes related to extracellular matrix, glycolysis, and neural development also increase. They may engage in adaptation and remodeling to the damaged tissue.

Conclusions

Mechanisms of 5AzC-induced toxicity and repair process in the developing fetal brain were examined from the multiple viewpoints in the present study. I exposed pregnant rat on day 13 or mouse on day 12 of gestation to 5AzC and used the exposed fetal brain for the analyses. The obtained results were as follows.

In chapter 1, 5AzC-induced toxicity to the developing neural cells was examined, focusing on the effects on apoptosis and cell cycle kinetics. 5AzC first induced the accumulation of cells showing abnormal mitosis, G2 phase arrest, and then apoptosis of the neural progenitor cells, from 6 h to 24 h after 5AzC-treatment. Most of the apoptotic cells were in G1 phase. Further the nuclear migration of neural progenitor cells that is closely related to cell cycle progression delayed as compared to the control migration, and paralleled with cell cycle arrest. The present results indicate that 5AzC induced apoptosis and cell cycle arrest to the neural cells in the developing brain, which would lead to malformations in the neonatal brain.

For clarifying the molecular mechanisms of 5AzC-induced toxicity in the fetal brains, in chapter 2, DNA microarray analysis was undertaken to find genes that regulate cell death and cell cycle arrest. I then focused on the role of tumor suppressor protein p53, which plays a critical role in response to DNA damage. p53 protein and its target genes mRNAs and proteins increased and were expressed in the VZ, synchronized with the appearance of apoptotic cells. In p53-deficient fetal brains, apoptosis did not occur, although G2/M arrest was induced, suggesting that apoptosis is p53-dependent, but that another mechanism governs the G2/M checkpoint. The G2/M regulator, Cdc2, was activated by dephosphorylation through G2/M accumulation,

suggesting that accelerated entry into mitosis lead to accumulation of cells showing abnormal mitosis. The results revealed that the neural progenitor cells use several molecular mechanisms to regulate cell cycle progression and cell death toward the extrinsic stresses.

In chapter 3, to clarify how the developing brain responds and adapts to the damaged tissue, the repair process after the 5AzC-induced injury was examined. Histological examination and cell cycle analysis showed that repair process was completed around 60 h after treatment. During the repair period, a number of amoeboid microglia infiltrated the brain and ingested the apoptotic cells. DNA microarray analysis showed the upregulation of genes relevant to glial cells, inflammation, the extracellular matrix, glycolysis, proliferation, and neural development. Thus, it was shown here that the developing brain has the capacity to respond to the damage induced by extrinsic chemical stresses, including changing the expression of numerous genes and the induction of microglia to aid the repair process.

In conclusion, 5AzC induces toxicity and injury into the developing fetal brain via cell death which is mediated by p53, and disruption of normal proliferation by cell cycle arrest which occurs by p53-independent manner. Further the developing brain repairs the 5AzC-induced injuries with expressing various genes and the aid of microglial cells. It is supposed that the degree of damage induced by extrinsic stresses, and the extent of the subsequent repair process, would dramatically influence the level of abnormalities that would come in the neonatal brain.

Fetal neural damage is an important issue affecting the completion of normal

development of the CNS. A large number of processes, i.e. proliferation, migration, differentiation, and axon projection, are possibly affected by the extrinsic stresses during the development. Recently, brain science progresses to a great extent, and many concepts about the brain development have been revealed. To clarify the mechanism of fetal CNS toxicity induced by environmental factors, therefore, it is needed to compare the defects in brain development carefully and correctly with the mechanism of normal brain development. Further works on the fetal brain damages induced by various extrinsic stresses will reveal the factors which are important for brain development and its disorders. I hope that the present study offers important insights into the mechanisms of CNS development disorders and contributes to resolve the problems that affect the normal brain development.

References

Alliot F, Godin I, Pessac B. 1999. Microglia derive from progenitors, originating from the yolk sac, and which proliferate in the brain. Brain Res Dev Brain Res 117:145-152.

Altmann CR, Brivanlou AH. 2001. Neural patterning in the vertebrate embryo. Int Rev Cytol 203:447-482.

Angevine JB, Sidman RL. 1961. Autoradiographic study of cell migration during histogenesis of cerebral cortex in the mouse. Nature 192:766-768.

Ashwell K. 1991. The distribution of microglia and cell death in the fetal rat forebrain. Brain Res Dev Brain Res 58:1-12.

Bansal R, Lakhina V, Remedios R, Tole S. 2003. Expression of FGF receptors 1, 2, 3 in the embryonic and postnatal mouse brain compared with Pdgfralpha, Olig2 and Plp/dm20: implications for oligodendrocyte development. Dev Neurosci 25:83-95.

Bayer SA, Altman J. 1995. Neurogenesis and neuronal migration. In: The rat nervous system. 2nd ed. Paxinos G. Academic press. San Diego. pp1070-1074.

Bender CM, Pao MM, Jones PA. 1998. Inhibition of DNA methylation by 5-aza-2'-deoxycytidine suppresses the growth of human tumor cell lines. Cancer Res 58:95-101.

Besson A, Gurian-West M, Schmidt A, Hall A, Roberts JM. 2004. p27Kip1 modulates cell migration through the regulation of RhoA activation. Genes Dev 18:862-876.

Blaschke AJ, Staley K, Chun J. 1996. Widespread programmed cell death in proliferative and postmitotic regions of the fetal cerebral cortex. Development 122:1165-1174.

Bolaris S, Bozas E, Benekou A, Philippidis H, Stylianopoulou F. 2001. In utero radiation-induced apoptosis and p53 gene expression in the developing rat brain. Int J Rad Biol 77:71-81.

Borovitskaya AE, Evtushenko VI, Sabol SL. 1996. Gamma-radiation-induced cell death in the fetal rat brain possesses molecular characteristics of apoptosis and is associated with specific messenger RNA elevations. Brain Res Mol Brain Res 35:19-30.

Bracken CP, Whitelaw ML, Peet DJ. 2003. The hypoxia-inducible factors: key transcriptional regulators of hypoxic responses. Cell Mol Life Sci 60:1376-1393.

Burns TF, Fei P, Scata KA, Dicker DT, El-Deiry WS. 2003. Silencing of the novel p53 target gene Snk/Plk2 leads to mitotic catastrophe in paclitaxel (taxol)-exposed cells. Mol Cell Biol 23:5556-5571.

Calandra T, Roger T. 2003. Macrophage migration inhibitory factor: a regulator of innate immunity. Nat Rev Immunol 3:791-800.

Castedo M, Perfettini JL, Roumier T, Andreau K, Medema R, Kroemer G. 2004. Cell death by mitotic catastrophe: a molecular definition. Oncogene 23:2825-2837.

Charache S, Dover G, Smith K, Talbot CC, Jr., Moyer M, Boyer S. 1983. Treatment of sickle cell anemia with 5-azacytidine results in increased fetal hemoglobin production and is associated with nonrandom hypomethylation of DNA around the gamma-delta-beta-globin gene complex. Proc Natl Acad Sci U S A 80:4842-4846.

Chaturvedi P, Eng WK, Zhu Y, Mattern MR, Mishra R, Hurle MR, Zhang X, Annan RS, Lu Q, Faucette LF, Scott GF, Li X, Carr SA, Johnson RK, Winkler JD, Zhou BB. 1999. Mammalian Chk2 is a downstream effector of the ATM-dependent DNA damage checkpoint pathway. Oncogene 18:4047-4054.

Chenn A, Walsh CA. 2002. Regulation of cerebral cortical size by control of cell cycle exit in neural precursors. Science 297:365-369.

Cheville NF. 1994. Neoplasia: neoplastic cell structure. In: Ultrastructural pathology: an introduction to interpretation. Cheville NF. Ames: Iowa State University Press. Ames. pp234-251.

Choi JS, Cha JH, Park HJ, Chung JW, Chun MH, Lee MY. 2004. Transient expression of osteopontin mRNA and protein in amoeboid microglia in developing rat brain. Exp Brain Res 154:275-280.

Claus R, Almstedt M, Lubbert M. 2005. Epigenetic treatment of hematopoietic malignancies: in vivo targets of demethylating agents. Semin Oncol 32:511-520.

Constantinides PG, Jones PA, Gevers W. 1977. Functional striated muscle cells from non-myoblast precursors following 5-azacytidine treatment. Nature 267:364-366.

Costa LG, Aschner M, Vitalone A, Syversen T, Soldin OP. 2004. Developmental neuropathology of environmental agents. Annu Rev Pharmacol Toxicol 44:87-110.

Cross SM, Sanchez CA, Morgan CA, Schimke MK, Ramel S, Idzerda RL, Raskind WH, Reid BJ. 1995. A p53-dependent mouse spindle checkpoint. Science 267:1353-1356.

Cuadros MA, Navascues J. 1998. The origin and differentiation of microglial cells during development. Prog Neurobiol 56:173-189.

D'Sa C, Klocke BJ, Cecconi F, Lindsten T, Thompson CB, Korsmeyer SJ, Flavell RA, Roth KA. 2003. Caspase regulation of genotoxin-induced neural precursor cell death. J Neurosci Res 74:435-445.

D'Sa-Eipper C, Roth KA. 2000. Caspase regulation of neuronal progenitor cell apoptosis. Dev Neurosci 22:116-124.

Diez-Juan A, Andres V. 2003. Coordinate control of proliferation and migration by the

p27Kip1/cyclin-dependent kinase/retinoblastoma pathway in vascular smooth muscle cells and fibroblasts. Circ Res 92:402-410.

Dodge JE, Okano M, Dick F, Tsujimoto N, Chen T, Wang S, Ueda Y, Dyson N, Li E. 2005. Inactivation of Dnmt3b in mouse embryonic fibroblasts results in DNA hypomethylation, chromosomal instability, and spontaneous immortalization. J Biol Chem 280:17986-17991.

Doetsch F. 2003. The glial identity of neural stem cells. Nat Neurosci 6:1127-1134.

Dou CL, Li S, Lai E. 1999. Dual role of brain factor-1 in regulating growth and patterning of the cerebral hemispheres. Cereb Cortex 9:543-550.

Dulic V, Kaufmann WK, Wilson SJ, Tlsty TD, Lees E, Harper JW, Elledge SJ, Reed SI. 1994. p53-dependent inhibition of cyclin-dependent kinase activities in human fibroblasts during radiation-induced G1 arrest. Cell 76:1013-1023.

Egger G, Liang G, Aparicio A, Jones PA. 2004. Epigenetics in human disease and prospects for epigenetic therapy. Nature 429:457-463.

Eisenstat DD, Liu JK, Mione M, Zhong W, Yu G, Anderson SA, Ghattas I, Puelles L, Rubenstein JL. 1999. DLX-1, DLX-2, and DLX-5 expression define distinct stages of basal forebrain differentiation. J Comp Neurol 414:217-237.

el-Deiry WS, Tokino T, Velculescu VE, Levy DB, Parsons R, Trent JM, Lin D, Mercer WE, Kinzler KW, Vogelstein B. 1993. WAF1, a potential mediator of p53 tumor suppression. Cell 75:817-825.

Fan G, Martinowich K, Chin MH, He F, Fouse SD, Hutnick L, Hattori D, Ge W, Shen Y, Wu H, ten Hoeve J, Shuai K, Sun YE. 2005. DNA methylation controls the timing of astrogliogenesis through regulation of JAK-STAT signaling. Development 132:3345-3356.

Fawcett JW, Asher RA. 1999. The glial scar and central nervous system repair. Brain Res Bull 49:377-391.

Ferguson AT, Vertino PM, Spitzner JR, Baylin SB, Muller MT, Davidson NE. 1997. Role of estrogen receptor gene demethylation and DNA methyltransferase.DNA adduct formation in 5-aza-2'deoxycytidine-induced cytotoxicity in human breast cancer cells. J Biol Chem 272:32260-32266.

Flagiello D, Bernardino-Sgherri J, Dutrillaux B. 2002. Complex relationships between 5-aza-dC induced DNA demethylation and chromosome compaction at mitosis. Chromosoma 111:37-44.

Fujita S. 1960. Mitotic pattern and histogenesis of the central nervous system. Nature 185:702-703.

Fujita S. 1962. Kinetics of cellular proliferation. Exp Cell Res 28:52-60.

Fujita S. 1963. The matrix cell and cytogenesis in the developing central nervous system. J Comp Neurol 120:37-42.

Fujita S. 2003. The discovery of the matrix cell, the identification of the multipotent neural stem cell

and the development of the central nervous system. Cell Struct Funct 28:205-228.

Fukui R, Shibata N, Kohbayashi E, Amakawa M, Furutama D, Hoshiga M, Negoro N, Nakakouji T, Ii M, Ishihara T, Ohsawa N. 1997. Inhibition of smooth muscle cell migration by the p21 cyclin-dependent kinase inhibitor (Cip1). Atherosclerosis 132:53-59.

Furukawa S, Abe M, Usuda K, Ogawa I. 2004. Indole-3-acetic acid induces microencephaly in rat fetuses. Toxicol Pathol 32:659-667.

Galceran J, Miyashita-Lin EM, Devaney E, Rubenstein JL, Grosschedl R. 2000. Hippocampus development and generation of dentate gyrus granule cells is regulated by LEF1. Development 127:469-482.

Gao Y, Sun Y, Frank KM, Dikkes P, Fujiwara Y, Seidl KJ, Sekiguchi JM, Rathbun GA, Swat W, Wang J, Bronson RT, Malynn BA, Bryans M, Zhu C, Chaudhuri J, Davidson L, Ferrini R, Stamato T, Orkin SH, Greenberg ME, Alt FW. 1998. A critical role for DNA end-joining proteins in both lymphogenesis and neurogenesis. Cell 95:891-902.

Gavrieli Y, Sherman Y, Ben-Sasson SA. 1992. Identification of programmed cell death in situ via specific labeling of nuclear DNA fragmentation. J Cell Biol 119:493-501.

Gimeno L, Brulet P, Martinez S. 2003. Study of Fgf15 gene expression in developing mouse brain. Gene Expr Patterns 3:473-481.

Gorczyca W, Gong J, Darzynkiewicz Z. 1993. Detection of DNA strand breaks in individual apoptotic cells by the in situ terminal deoxynucleotidyl transferase and nick translation assays. Cancer Res 53:1945-1951.

Gross A, Jockel J, Wei MC, Korsmeyer SJ. 1998. Enforced dimerization of BAX results in its translocation, mitochondrial dysfunction and apoptosis. EMBO J 17:3878-3885.

Grove EA, Fukuchi-Shimogori T. 2003. Generating the cerebral cortical area map. Annu Rev Neurosci 26:355-380.

Gumbiner BM. 2005. Regulation of cadherin-mediated adhesion in morphogenesis. Nat Rev Mol Cell Biol 6:622-634.

Hanisch UK. 2002. Microglia as a source and target of cytokines. Glia 40:140-155.

Hao AJ, Dheen ST, Ling EA. 2001. Response of amoeboid microglia/brain macrophages in fetal rat brain exposed to a teratogen. J Neurosci Res 64:79-93.

Hao AJ, Dheen ST, Ling EA. 2001. Induction of cytokine expression in the brain macrophages/amoeboid microglia of the fetal rat exposed to a teratogen. Neuroreport 12:1391-1397.

Hao AJ, Dheen ST, Ling EA. 2002. Expression of macrophage colony-stimulating factor and its receptor in microglia activation is linked to teratogen-induced neuronal damage. Neuroscience

112:889-900.

Hartfuss E, Galli R, Heins N, Gotz M. 2001. Characterization of CNS precursor subtypes and radial glia. Dev Biol 229:15-30.

He TC, Sparks AB, Rago C, Hermeking H, Zawel L, da Costa LT, Morin PJ, Vogelstein B, Kinzler KW. 1998. Identification of c-MYC as a target of the APC pathway. Science 281:1509-1512.

Henderson DW, Papadimitriou JM. 1982. The neoplastic cell I: nuclear ultrastructure. In: Ultrastructural appearances of tumors: a diagnostic atlas. Henderson DW, Papadimitriou JM. Churchill Livingstone. New York. pp11-29.

Hossain MM, Nakayama H, Goto N. 1995. Apoptosis in the central nervous system of developing mouse fetuses from 5-azacytidine-administered dams. Toxicol Pathol 23:367-372.

Houle J, Das G. 1983. Tissue repair in the embryonic rat spinal cord following exposure to N-ethyl-N-nitrosourea. Int J Dev Neurosci 2:1-7.

Iliakis G, Wang Y, Guan J, Wang H. 2003. DNA damage checkpoint control in cells exposed to ionizing radiation. Oncogene 22:5834-5847.

Imai Y, Kohsaka S. 2002. Intracellular signaling in M-CSF-induced microglia activation: role of Iba1. Glia 40:164-174.

Itoh N, Yonehara S, Ishii A, Yonehara M, Mizushima S, Sameshima M, Hase A, Seto Y, Nagata S. 1991. The polypeptide encoded by the cDNA for human cell surface antigen Fas can mediate apoptosis. Cell 66:233-243.

Jackson-Grusby L, Beard C, Possemato R, Tudor M, Fambrough D, Csankovszki G, Dausman J, Lee P, Wilson C, Lander E, Jaenisch R. 2001. Loss of genomic methylation causes p53-dependent apoptosis and epigenetic deregulation. Nat Genet 27:31-39.

Johnson DE, Williams LT. 1993. Structural and functional diversity in the FGF receptor multigene family. Adv Cancer Res 60:1-41.

Jones PA, Taylor SM. 1980. Cellular differentiation, cytidine analogs and DNA methylation. Cell 20:85-93.

Juttermann R, Li E, Jaenisch R. 1994. Toxicity of 5-aza-2'-deoxycytidine to mammalian cells is mediated primarily by covalent trapping of DNA methyltransferase rather than DNA demethylation. Proc Natl Acad Sci U S A 91:11797-11801.

Karpf AR, Moore BC, Ririe TO, Jones DA. 2001. Activation of the p53 DNA damage response pathway after inhibition of DNA methyltransferase by 5-aza-2'-deoxycytidine. Mol Pharmacol 59:751-757.

Kastan MB, Zhan Q, el-Deiry WS, Carrier F, Jacks T, Walsh WV, Plunkett BS, Vogelstein B,

Fornace AJ, Jr. 1992. A mammalian cell cycle checkpoint pathway utilizing p53 and GADD45 is defective in ataxia-telangiectasia. Cell 71:587-597.

Katayama K, Ishigami N, Suzuki M, Ohtsuka R, Kiatipattanasakul W, Nakayama H, Doi K. 2000. Teratologic studies on rat perinates and offspring from dams treated with ethylnitrosourea (ENU). Exp Anim 49:181-187.

Katayama K, Uetsuka K, Ishigami N, Nakayama H, Doi K. 2001. Apoptotic cell death and cell proliferative activity in the rat fetal central nervous system from dams administered with ethylnitrosourea (ENU). Histol Histopathol 16:79-85.

Katayama K, Ohtsuka R, Takai H, Nakayama H, Doi K. 2002. Expression of p53 and its transcriptional target genes mRNAs in the ethylnitrosourea-induced apoptosis and cell cycle arrest in the fetal central nervous system. Histol Histopathol 17:715-720.

Katayama K, Ueno M, Yamauchi H, Nagata T, Nakayama H, Doi K. 2005. Ethylnitrosourea induces neural progenitor cell apoptosis after S-phase accumulation in a p53-dependent manner. Neurobiol Dis 18:218-225.

Katayama K, Ueno M, Yamauchi H, Nakayama H, Doi K. 2005. Microarray analysis of genes in fetal central nervous system after ethylnitrosourea administration. Birth Defects Res B Dev Reprod Toxicol 74:255-260.

Kaur C, Hao AJ, Wu CH, Ling EA. 2001. Origin of microglia. Microsc Res Tech 54:2-9.

Keramaris E, Stefanis L, MacLaurin J, Harada N, Takaku K, Ishikawa T, Taketo MM, Robertson GS, Nicholson DW, Slack RS, Park DS. 2000. Involvement of caspase 3 in apoptotic death of cortical neurons evoked by DNA damage. Mol Cell Neurosci 15:368-379.

Kikuchi-Horie K, Kawakami E, Kamata M, Wada M, Hu JG, Nakagawa H, Ohara K, Watabe K, Oyanagi K. 2004. Distinctive expression of midkine in the repair period of rat brain during neurogenesis: immunohistochemical and immunoelectron microscopic observations. J Neurosci Res 75:678-687.

Kitamura M, Itoh K, Matsumoto A, Hayashi Y, Sasaki R, Imai Y, Itoh H. 2001. Prenatal ionizing radiation-induced apoptosis of the developing murine brain with special references to the expression of some proteins. Kobe J Med Sci 47:59-76.

Kops GJ, Weaver BA, Cleveland DW. 2005. On the road to cancer: aneuploidy and the mitotic checkpoint. Nat Rev Cancer 5:773-785.

Kuida K, Zheng TS, Na S, Kuan C, Yang D, Karasuyama H, Rakic P, Flavell RA. 1996. Decreased apoptosis in the brain and premature lethality in CPP32-deficient mice. Nature 384:368-372.

Lakin ND, Jackson SP. 1999. Regulation of p53 in response to DNA damage. Oncogene 18:7644-

7655.

Langman J, Guerrant RL, Freeman BG. 1966. Behavior of neuro-epithelial cells during closure of the neural tube. Journal of Comparative Neurology 127:399-411.

Langman J, Shimada M. 1971. Cerebral cortex of the mouse after prenatal chemical insult. Am J Anat 132:355-374.

Lanni JS, Jacks T. 1998. Characterization of the p53-dependent postmitotic checkpoint following spindle disruption. Mol Cell Biol 18:1055-1064.

Ley TJ, DeSimone J, Anagnou NP, Keller GH, Humphries RK, Turner PH, Young NS, Keller P, Nienhuis AW. 1982. 5-azacytidine selectively increases gamma-globin synthesis in a patient with beta+ thalassemia. New Eng J Med 307:1469-1475.

Liu Q, Guntuku S, Cui XS, Matsuoka S, Cortez D, Tamai K, Luo G, Carattini-Rivera S, DeMayo F, Bradley A, Donehower LA, Elledge SJ. 2000. Chk1 is an essential kinase that is regulated by Atr and required for the G(2)/M DNA damage checkpoint. Genes Dev 14:1448-1459.

Lu DP, Nakayama H, Shinozuka J, Uetsuka K, Taki R, Doi K. 1998. 5-Azacytidine-induced apoptosis in the central nervous system of developing rat fetuses. J Tox Path 11:133-136.

Magavi SS, Leavitt BR, Macklis JD. 2000. Induction of neurogenesis in the neocortex of adult mice. Nature 405:951-955.

Mateos S, Dominguez I, Pastor N, Cantero G, Cortes F. 2005. The DNA demethylating 5-azaC induces endoreduplication in cultured Chinese hamster cells. Mutat Res 578:33-42.

Matsuoka S, Rotman G, Ogawa A, Shiloh Y, Tamai K, Elledge SJ. 2000. Ataxia telangiectasia-mutated phosphorylates Chk2 in vivo and in vitro. Proc Natl Acad Sci U S A 97:10389-10394.

May P, May E. 1999. Twenty years of p53 research: structural and functional aspects of the p53 protein. Oncogene 18:7621-7636.

Mendola P, Selevan SG, Gutter S, Rice D. 2002. Environmental factors associated with a spectrum of neurodevelopmental deficits. Ment Retard Dev Disabil Res Rev 8:188-197.

Michalowsky LA, Jones PA. 1987. Differential nuclear protein binding to 5-azacytosine-containing DNA as a potential mechanism for 5-aza-2'-deoxycytidine resistance. Mol Cell Biol 7:3076-3083.

Michiels C. 2004. Physiological and pathological responses to hypoxia. Am J Pathol 164:1875-1882.

Miyata T, Kawaguchi A, Okano H, Ogawa M. 2001. Asymmetric inheritance of radial glial fibers by cortical neurons. Neuron 31:727-741.

Miyata T, Kawaguchi A, Saito K, Kawano M, Muto T, Ogawa M. 2004. Asymmetric production of surface-dividing and non-surface-dividing cortical progenitor cells. Development 131:3133-3145.

Monuki ES, Porter FD, Walsh CA. 2001. Patterning of the dorsal telencephalon and cerebral cortex

by a roof plate-Lhx2 pathway. Neuron 32:591-604.

Muller M, Wilder S, Bannasch D, Israeli D, Lehlbach K, Li-Weber M, Friedman SL, Galle PR, Stremmel W, Oren M, Krammer PH. 1998. p53 activates the CD95 (APO-1/Fas) gene in response to DNA damage by anticancer drugs. J Exp Med 188:2033-2045.

Murakami T, Li X, Gong J, Bhatia U, Traganos F, Darzynkiewicz Z. 1995. Induction of apoptosis by 5-azacytidine: drug concentration-dependent differences in cell cycle specificity. Cancer Res 55:3093-3098.

Nagata S, Golstein P. 1995. The Fas death factor. Science 267:1449-1456.

Nakajima K, Kohsaka S. 2001. Microglia: activation and their significance in the central nervous system. J Biochem 130:169-175.

Namihira M, Nakashima K, Taga T. 2004. Developmental stage dependent regulation of DNA methylation and chromatin modification in a immature astrocyte specific gene promoter. FEBS Lett 572:184-188.

Nieto M, Samper E, Fraga MF, Gonzalez de Buitrago G, Esteller M, Serrano M. 2004. The absence of p53 is critical for the induction of apoptosis by 5-aza-2'-deoxycytidine. Oncogene 23:735-743.

Niida H, Tsuge S, Katsuno Y, Konishi A, Takeda N, Nakanishi M. 2005. Depletion of Chk1 leads to premature activation of cdc2-cyclin B and mitotic catastrophy. J Biol Chem 13:13.

Nitta M, Kobayashi O, Honda S, Hirota T, Kuninaka S, Marumoto T, Ushio Y, Saya H. 2004. Spindle checkpoint function is required for mitotic catastrophe induced by DNA-damaging agents. Oncogene 23:6548-6558.

Noctor SC, Flint AC, Weissman TA, Dammerman RS, Kriegstein AR. 2001. Neurons derived from radial glial cells establish radial units in neocortex. Nature 409:714-720.

Noctor SC, Martinez-Cerdeno V, Ivic L, Kriegstein AR. 2004. Cortical neurons arise in symmetric and asymmetric division zones and migrate through specific phases. Nat Neurosci 7:136-144.

Ohtsuka T, Jensen MR, Kim HG, Kim KT, Lee SW. 2004. The negative role of cyclin G in ATM-dependent p53 activation. Oncogene 23:5405-5408.

Oka M, Meacham AM, Hamazaki T, Rodic N, Chang LJ, Terada N. 2005. De novo DNA methyltransferases Dnmt3a and Dnmt3b primarily mediate the cytotoxic effect of 5-aza-2'-deoxycytidine. Oncogene 24:3091-3099.

Okamoto K, Beach D. 1994. Cyclin G is a transcriptional target of the p53 tumor suppressor protein. EMBO J 13:4816-4822.

Okamoto K, Li H, Jensen MR, Zhang T, Taya Y, Thorgeirsson SS, Prives C. 2002. Cyclin G recruits PP2A to dephosphorylate Mdm2. Mol Cell 9:761-771.

Oppenheim RW. 1991. Cell death during development of the nervous system. Annu Rev Neurosci 14:453-501.

Oyanagi K, Kakita A, Yamada M, Kawasaki K, Hayashi S, Ikuta F. 1998. Process of repair in the neuroepithelium of developing rat brain during neurogenesis: chronological and quantitative observation of DNA-replicating cells. Brain Res Dev Brain Res 108:229-238.

Qian X, Shen Q, Goderie SK, He W, Capela A, Davis AA, Temple S. 2000. Timing of CNS cell generation: a programmed sequence of neuron and glial cell production from isolated murine cortical stem cells. Neuron 28:69-80.

Rakic P. 1988. Specification of cerebral cortical areas. Science 241:170-176.

Rao MS. 1999. Multipotent and restricted precursors in the central nervous system. Anat Rec 257:137-148.

Raska K, Jurovcik M, Sormova Z. 1965. On the metabolism of 5-azacytidine and 5-aza-2-eoxycytidine in mice. Collect Czech Chem Commun 30:3001-3006.

Rodier PM, Reynolds SS, Roberts WN. 1979. Behavioral consequences of interference with CNS development in the early fetal period. Teratology 19:327-336.

Rodier PM. 1995. Developing brain as a target of toxicity. Environ Health Perspect 103:73-76.

Rubenstein JL, Shimamura K, Martinez S, Puelles L. 1998. Regionalization of the prosencephalic neural plate. Annu Rev Neurosci 21:445-477.

Sablina AA, Agapova LS, Chumakov PM, Kopnin BP. 1999. p53 does not control the spindle assembly cell cycle checkpoint but mediates G1 arrest in response to disruption of microtubule system. Cell Biol Int 23:323-334.

Saitsu H, Komada M, Suzuki M, Nakayama R, Motoyama J, Shiota K, Ishibashi M. 2005. Expression of the mouse Fgf15 gene is directly initiated by Sonic hedgehog signaling in the diencephalon and midbrain. Dev Dyn 232:282-292.

Salie R, Niederkofler V, Arber S. 2005. Patterning molecules; multitasking in the nervous system. Neuron 45:189-192.

Sano H, Hsu DK, Apgar JR, Yu L, Sharma BB, Kuwabara I, Izui S, Liu FT. 2003. Critical role of galectin-3 in phagocytosis by macrophages. J Clin Invest 112:389-397.

Santi DV, Norment A, Garrett CE. 1984. Covalent bond formation between a DNA-cytosine methyltransferase and DNA containing 5-azacytosine. Proc Natl Acad Sci U S A 81:6993-6997.

Sauer ME, Walker BE. 1959. Radioautographic study of interkinetic nuclear migration in the neural tube. Proc Soc Exp Biol Med 101:557-560.

Schmahl W, Torok P, Kriegel H. 1984. Embryotoxicity of 5-azacytidine in mice. Phase- and dose-

specificity studies. Arch Toxicol 55:143-147.

Seifertova M, Vesely J, Sorm F. 1968. Effect of 5-azacytidine on developing mouse embryo. Experientia 24:487-488.

Seifertova M, Vesely J, Cihak A. 1974. Localization of the labelled 5-azacytidine in cultured mouse embryonic cells. Experientia 30:1463-1465.

Selvakumaran M, Lin HK, Miyashita T, Wang HG, Krajewski S, Reed JC, Hoffman B, Liebermann D. 1994. Immediate early up-regulation of bax expression by p53 but not TGF beta 1: a paradigm for distinct apoptotic pathways. Oncogene 9:1791-1798.

Semont A, Nowak EB, Silva Lages C, Mathieu C, Mouthon MA, May E, Allemand I, Millet P, Boussin FD. 2004. Involvement of p53 and Fas/CD95 in murine neural progenitor cell response to ionizing irradiation. Oncogene 13:1-12.

Sheng HZ, Bertuzzi S, Chiang C, Shawlot W, Taira M, Dawid I, Westphal H. 1997. Expression of murine Lhx5 suggests a role in specifying the forebrain. Dev Dyn 208:266-277.

Shimada M, Langman J. 1970. Repair of the external granular layer of the hamster cerebellum after prenatal and postnatal administration of methylazoxymethanol. Teratology 3:119-133.

Shtutman M, Zhurinsky J, Simcha I, Albanese C, D'Amico M, Pestell R, Ben-Ze'ev A. 1999. The cyclin D1 gene is a target of the beta-catenin/LEF-1 pathway. Proc Natl Acad Sci U S A 96:5522-5527.

Smith ML, Chen IT, Zhan Q, Bae I, Chen CY, Gilmer TM, Kastan MB, O'Connor PM, Fornace AJ, Jr. 1994. Interaction of the p53-regulated protein Gadd45 with proliferating cell nuclear antigen. Science 266:1376-1380.

Sorokin SP, Hoyt RF, Jr., Blunt DG, McNelly NA. 1992. Macrophage development: II. Early ontogeny of macrophage populations in brain, liver, and lungs of rat embryos as revealed by a lectin marker. Anat Rec 232:527-550.

Sun XZ, Takahashi S, Fukui Y, Hisano S, Kuboda Y, Sato H, Inouye M. 1999. Different patterns of abnormal neuronal migration in the cerebral cortex of mice prenatally exposed to irradiation. Brain Res Dev Brain Res 114:99-108.

Sun J, Marx SO, Chen HJ, Poon M, Marks AR, Rabbani LE. 2001. Role for p27(Kip1) in Vascular Smooth Muscle Cell Migration. Circulation 103:2967-2972.

Sun YE, Martinowich K, Ge W. 2003. Making and repairing the mammalian brain--signaling toward neurogenesis and gliogenesis. Semin Cell Dev Biol 14:161-168.

Takahashi T, Nowakowski RS, Caviness VS, Jr. 1992. BUdR as an S-phase marker for quantitative studies of cytokinetic behaviour in the murine cerebral ventricular zone. J Neurocytol 21:185-197.

Takahashi T, Nowakowski RS, Caviness VS, Jr. 1993. Cell cycle parameters and patterns of nuclear movement in the neocortical proliferative zone of the fetal mouse. J Neurosci 13:820-833.

Takahashi T, Nowakowski RS, Caviness VS, Jr. 1995. The cell cycle of the pseudostratified ventricular epithelium of the embryonic murine cerebral wall. J Neurosci 15:6046-6057.

Takeichi M. 1995. Morphogenetic roles of classic cadherins. Curr Opin Cell Biol 7:619-627.

Takizawa T, Nakashima K, Namihira M, Ochiai W, Uemura A, Yanagisawa M, Fujita N, Nakao M, Taga T. 2001. DNA methylation is a critical cell-intrinsic determinant of astrocyte differentiation in the fetal brain. Dev Cell 1:749-758.

Tamamaki N, Nakamura K, Okamoto K, Kaneko T. 2001. Radial glia is a progenitor of neocortical neurons in the developing cerebral cortex. Neurosci Res 41:51-60.

Taylor WR, Stark GR. 2001. Regulation of the G2/M transition by p53. Oncogene 20:1803-1815.

Temple S. 2001. The development of neural stem cells. Nature 414:112-117.

Tetsu O, McCormick F. 1999. Beta-catenin regulates expression of cyclin D1 in colon carcinoma cells. Nature 398:422-426.

Thomaidou D, Mione MC, Cavanagh JF, Parnavelas JG. 1997. Apoptosis and its relation to the cell cycle in the developing cerebral cortex. J Neurosci 17:1075-1085.

Timme TL, Thompson TC. 1994. Rapid allelotype analysis of p53 knockout mice. Biotechniques 17:460, 462-463.

Timonen S, Therman E. 1950. The changes in the mitotic mechanism of human cancer cells. Cancer Res 10:431-439.

Ueno M, Katayama K, Nakayama H, Doi K. 2002. Mechanisms of 5-azacytidine (5AzC)-induced toxicity in the rat foetal brain. Int J Exp Pathol 83:139-150.

Ueno M, Katayama K, Yasoshima A, Nakayama H, Doi K. 2002. 5-Azacytidine (5AzC)-induced histopathological changes in the central nervous system of rat fetuses. Exp Toxicol Pathol 54:91-96.

Ueno M, Nakayama H, Kajikawa S, Katayama K, Suzuki K, Doi K. 2002. Expression of ribosomal protein L4 (rpL4) during neurogenesis and 5-azacytidine (5AzC)-induced apoptotic process in the rat. Histol Histopathol 17:789-798.

Ueno M, Katayama K, Yamauchi H, Nakayama H, Doi K. 2005. Cell cycle and cell death regulation of neural progenitor cells in the 5-azacytidine (5AzC)-treated developing fetal brain. Exp Neurol in press.

Vinson RK, Hales BF. 2002. DNA repair during organogenesis. Mutat Res 509:79-91.

Vlahovic M, Bulic-Jakus F, Juric-Lekic G, Fucic A, Maric S, Serman D. 1999. Changes in the placenta and in the rat embryo caused by the demethylating agent 5-azacytidine. Int J Dev Biol

43:843-846.

von Waechter R, Jaensch B. 1972. Generation times of the matrix cells during embryonic brain development: an autoradiographic study in rats. Brain Res 46:235-250.

Walther M, Kuklinski S, Pesheva P, Guntinas-Lichius O, Angelov DN, Neiss WF, Asou H, Probstmeier R. 2000. Galectin-3 is upregulated in microglial cells in response to ischemic brain lesions, but not to facial nerve axotomy. J Neurosci Res 61:430-435.

Yamauchi H, Katayama K, Ueno M, Uetsuka K, Nakayama H, Doi K. 2004. Involvement of p53 in 1-beta-D-arabinofuranosylcytosine-induced rat fetal brain lesions. Neurotoxicol Teratol 26:579-586.

Yoshida Y, Yamada M, Wakabayashi K, F. I. 1987. Immunohistochemical detection of DNA replicating cells in the developing nervous system: use of bromodeoxyuridine and its monoclonal antibody to rat fetuses. Biomed Res 8:431-444.

Zhang LL, Collier PA, Ashwell KW. 1995. Mechanisms in the induction of neuronal heterotopiae following prenatal cytotoxic brain damage. Neurotoxicol Teratol 17:297-311.

Zhou Q, Wang S, Anderson DJ. 2000. Identification of a novel family of oligodendrocyte lineage-specific basic helix-loop-helix transcription factors. Neuron 25:331-343.

Zhu WG, Hileman T, Ke Y, Wang P, Lu S, Duan W, Dai Z, Tong T, Villalona-Calero MA, Plass C, Otterson GA. 2004. 5-aza-2'-deoxycytidine activates the p53/p21Waf1/Cip1 pathway to inhibit cell proliferation. J Biol Chem 279:15161-15166.

Acknowledgements

I wish to express my appreciation to Professor Kunio Doi and Associate Professor Hiroyuki Nakayama for their encouragement and advice throughout the experiments, and all members in Department of Veterinary Pathology, especially, Mr. Kei-ichi Katayama, Mr. Hirofumi Yamauchi, and Mr. Takashi Mikami for their kind technical help and experimental advice. I am also grateful to Mr. Akira Yasoshima for his kind technical help on electron microscopy.

Finally, I wish to express all my gratitude to my parents, my friends, and Miss Keiko Horiuchi, for their heartful supports and encouragement.